

The Gravitational Effects of Blood Flow in Irregular Stenosed Artery with Various Severity

Yan Bin Tan¹, Norzieha Mustapha²

¹Department of Mathematical Sciences, Faculty of Science, Universiti Teknologi Malaysia, 81310 UTM Johor Bahru, Johor, Malaysia.

²Faculty of Computer and Mathematical Sciences, Universiti Teknologi MARA, UiTM Kelantan, 18500 Machang, Kelantan.

norzieha864@kelantan.uitm.edu.my^{2*}

*Corresponding author

Abstract: The mathematical study investigates the influences of gravitational force in an artery segment on the various severity of the stenosis. Blood flow along the arterial segment is considered as incompressible Newtonian fluid. An unsteady two-dimensional nonlinear model is taken where the governing Navier-Stokes equations are added with significant gravity term. Marker and Cell (MAC) method based on finite difference approximations in a staggered grid is selected to solve the problem. Results obtained show that slight difference of areal occlusion percentage of severe stenosis in a vessel can lead to significant impacts on blood flow patterns. With the presence of the gravitational acceleration force, the pressure and axial velocity along the vessel is generally higher than without the gravitational force. Besides, the wall shear stress is lower and the recirculation region is smaller in the presence of gravitational force.

Keywords: Blood flow, gravity, severe stenosis, Newtonian fluid

1 Introduction

The gravitational force is a natural force which draws physical bodies to the earth due to their individual masses. The distribution of fluids in the human body is affected by this fundamental force. The pulmonary circulation is generally thought to be a largely passive circuit in which blood flow distribution is predominantly determined by the hydrostatic gradient due to gravity. This perspective has dominated both the interpretation and direction of studies related to pulmonary perfusion for the past three decades [1]. The association between gravity and regional blood flow was confirmed by changing in the direction or magnitude of gravity relative to the vertical axis of the lung [2-3].

For space programmes to be carried out safely, studies on physical changes during absence of weight are performed. In space activities, astronauts encounter a condition of microgravity, causing body fluids to distribute more to upper parts of the body which is very different from the condition with gravitation on earth [4]. However at launch and on return, hypergravity is frequently faced. These types of changes in blood flow velocity due to gravitational force may cause several health problems especially when there are unhealthy deposits in blood vessels [5-7]. Payne [5] carried out the analysis of the effects of gravity and wall thickness on blood flow behaviour. Navier-Stokes equations were derived with additional of gravitational term, gS , where g is the gravitational acceleration and S is the vessel slope. The equations are linked to a simple vessel wall model. The result showed that amplitude of the velocity pulse changes with slope. On the other hand, it is noticed that the acceleration of gravity does not vary only during space activities; even on the earth itself, there are various causes affecting gravitation, such as latitude, altitude, tidal effects, and so forth. For example, at the equator, gravity acceleration gives a value of 9.78m/s^2 but it becomes 9.832m/s^2 when shifted to the poles [8]. These facts prove that the gravitational force is significant to be considered in the mathematical studies on blood flow in cardiovascular system.

The cardiovascular system in human body consists of the heart and circulatory system, which functions in body protection, regulation and transportation. The heart pumps and produces a pressure gradient for blood to flow through network of blood vessels [9]. Among the vessels, artery is

responsible to carry oxygenated blood from the heart to other parts of the body. However, cardiovascular diseases have been noticed as one of the major illnesses all around the world such as stroke and atherosclerosis. The major factor of these illnesses is segmental narrowing of an artery, which is also called the arterial stenosis. The stenosis usually happens due to substances deposition or intravascular plaques because of unhealthy living conditions such as exposure to tobacco smoke, lack of physical activity and so on [10]. It is always followed by serious changes in blood flow, pressure distribution, wall shear stress, and flow resistance, which lead to blood flow disorders. Once arterial stenosis occurs, atherosclerotic plaques would protrude into lumen of blood vessels. Consequently, resistance is increased; hence blood flow is insufficient to reach every cell and this resists nutrient supplement. These could lead to widespread of health disorders which may then worsen to various illnesses. To more serious extent, these abnormalities in blood flow could contribute substantial fatal health risks. Hence, several medications are needed to cure the illnesses.

To identify the health conditions of blood vessel, invasive methods are commonly used in medical diagnoses. Doctors refer to the diagnosis results to give treatments accordingly, based on their knowledge and experiences. Since the essential aims of these measurement methods are to diagnose and find solutions to the illness, non-invasive measurements and modelling have become significant preferences in the medical profession [11]. Several theoretical and experimental studies by mean of blood flow characteristics with arterial stenosis were done, such as Deplano *et al.* [12], Ling and Atabek [13], Padmanabhan [14], Back *et al.* [15], Johnston and Kilpatrick [16], Chakravarty and Sannigrahi [17], Jung *et al.* [18], Mandal [19] and Mustapha *et al.* [20-22]. The studies present important results on several blood flow characteristics and flow patterns under different circumstances. On the other hand, severity of stenosis is one of the main factors affecting blood flow characteristics. In clinical study carried out by Uren *et al.* [23], when hyperaemia (a condition of excessive blood) occurs in human body, rate of blood flow would decrease if there is a stenosis with severity degree about 40 percent. Shear rate of the blood would likely increase with increment of stenosis severity. Besides, another stenosis or restenosis would probably occur if the first stenosis is severe enough. Hence, the effects of stenosis severity on blood flow are also an interesting aspect to be investigated.

In order to carry out diagnoses invasively, mathematical modelling on blood flow in stenosed arteries has been expected to be important in studies of arteriosclerotic plaques and the effects. Various studies formulated an unsteady nonlinear two-dimensional model. In this study, effects of gravitational acceleration and stenosis severity are investigated to see how blood flow patterns vary. Here, blood flow in a straight stenosed artery is modelled by axisymmetric Navier-Stokes equations; while the artery itself is assumed to be an elastic cylindrical tube composing of Newtonian fluid which is the blood. The geometry of stenosis chosen is an irregular stenosis in cylindrical artery vessels following data given by Back *et al.* [15], which was adapted from clinical profile where the roughness of real constricted blood vessel surface is described. Blood flow is assumed to be unsteady, two-dimensional, and incompressible. Walls of artery vessels are considered to be elastic and axisymmetric. The numerical method chosen in this study is the finite difference approximations based on Marker and Cell (MAC) method following a MATLAB coding accomplished by Mustapha *et al.* [22]. Several blood flow characteristics are investigated including the pressure drop, velocity profiles, wall shear stress, and also streamline of the streaming blood across the longitudinal section of the constricted artery.

2 Problem Formulation

In this study, the choice of stenosis geometry is based on a numerical data developed by Back *et al.* [15]. The data constructs an arterial segment with single irregular stenosis representing the rough surface imitating clinical profile of a constricted blood vessel. The primary numerical data was published and plotted to represent a mild stenosis as in Figure 1. The geometry is non-dimensionalised as to carry out computational analyses.

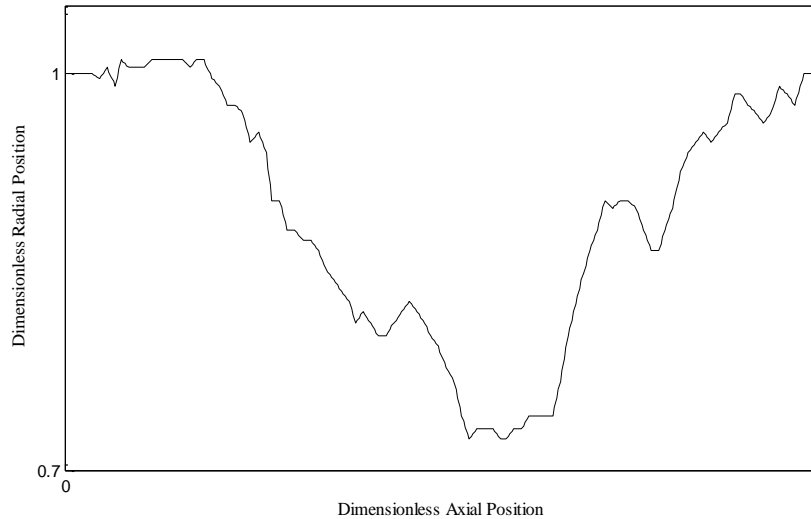


Figure 1: Geometry of Single Irregular Stenosis by Back *et al.* [15]

One of the common calculations to determine severity of a stenosis is by calculating the percentage of occlusion by diameter as follow:

$$\% \text{ occlusion} = \left(1 - \frac{D_{ste}^2}{D_{normal}^2} \right) \times 100 \quad (1)$$

where D_{ste} is the minimum lumen diameter as in stenotic arterial region under studied; while D_{normal} is the diameter of vessel without constriction as in region before and after occurrence of stenosis.

In this study, mild arterial stenosis is represented by arterial segment constriction of 48% occlusion which is developed from the numerical data provided by Back *et al.* [15]. Then, to visualise different level of stenosis severity, the geometry is modified to have 75% occlusion, 87% occlusion and 96% occlusion in the constricted artery segment, as shown in Figure 2 below. Throughout the paper, “severe stenosis” refers to stenosis with 96% occlusion.

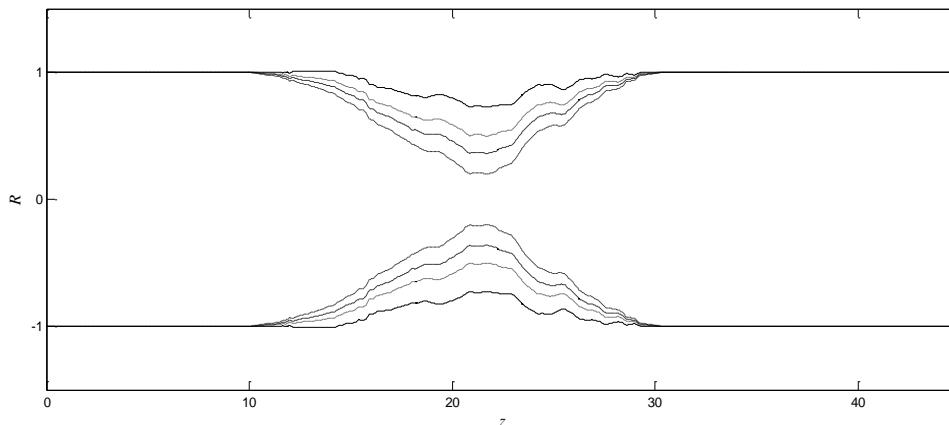


Figure 2: Cross-sectional Profile of the Single Irregular Stenosis Comparing Four Different Stages of Severity (48% occlusion, 75% occlusion, 87% occlusion and 96% occlusion)

To obtain a time-variant stenosis, the geometry data is multiplied by a time-variant parameter describing vessel wall motion:

$$a_1(t) = 1 + k_R \cos(\omega t - \phi) \quad (2)$$

where $\omega = 2\pi f_p$ is the angular frequency with f_p the pulse frequency, k_R is a constant and ϕ is the phase difference [20].

A few assumptions need to be made before proceeding to modelling of the problem. Blood flow in the constricted artery is accounted to be incompressible, two-dimensional, unsteady, laminar, fully developed and is modelled as Newtonian fluid. The fundamental governing fluid dynamics equations comprises of the Navier-Stokes Equations which are derived upon fundamental physics principles.

For convenience in the study of blood flow in constricted vessel, governing equations are written in cylindrical polar coordinates system (r, θ, z) . z conveys the longitudinal axis of the studied arterial segment while r conveys the radii along the region. Their respective velocity components are yielded by (u, v, w) . Conservative forms of the governing equations are:

$$\tilde{r} \frac{\partial \tilde{w}}{\partial \tilde{z}} + \frac{\partial(\tilde{u}\tilde{r})}{\partial \tilde{r}} = 0 \quad (3)$$

$$\frac{\partial \tilde{u}}{\partial \tilde{t}} + \frac{\partial \tilde{u}^2}{\partial \tilde{r}} + \frac{\partial(\tilde{w}\tilde{u})}{\partial \tilde{z}} + \frac{\tilde{u}^2}{\tilde{r}} = -\frac{1}{\rho} \frac{\partial \tilde{p}}{\partial \tilde{r}} + \nu \left(\frac{\partial^2 \tilde{u}}{\partial \tilde{r}^2} + \frac{1}{\tilde{r}} \frac{\partial \tilde{u}}{\partial \tilde{r}} + \frac{\partial^2 \tilde{u}}{\partial \tilde{z}^2} - \frac{\tilde{u}}{\tilde{r}^2} \right) + \rho g \sin \theta \quad (4)$$

$$\frac{\partial \tilde{w}}{\partial \tilde{t}} + \frac{\partial(\tilde{w}\tilde{u})}{\partial \tilde{r}} + \frac{\partial \tilde{w}^2}{\partial \tilde{z}} + \frac{\tilde{w}\tilde{u}}{\tilde{r}} = -\frac{1}{\rho} \frac{\partial \tilde{p}}{\partial \tilde{z}} + \nu \left(\frac{\partial^2 \tilde{w}}{\partial \tilde{r}^2} + \frac{1}{\tilde{r}} \frac{\partial \tilde{w}}{\partial \tilde{r}} + \frac{\partial^2 \tilde{w}}{\partial \tilde{z}^2} \right) - \rho g \cos \theta \quad (5)$$

Equation (3) is the continuity equation while equations (4) and (5) are radial and axial momentum equations respectively. ν represents the kinematic viscosity ($\frac{\mu}{\rho}$) of blood, ρ is the blood density and p represents pressure in the arterial segment.

Payne [5] suggested that gravity effects are negligible to radial momentum when compared to axial momentum. However during this study, the out-coming computational results show that there are light differences in some parameters when inserting gravity term at the radial momentum equation. Hence, the present study takes into consideration in imposing additional term of gravitational acceleration, $\mathbf{g} = (g \sin \theta, 0, -g \cos \theta)$, which involves both radial and axial momentum equations. Here, g is the gravitational acceleration and θ is the vertical angle between directions of vessel and gravity [24].

To carry out the numerical method of solution, the above parameters need to have the same dimension. Thus, non-dimensionalisation is performed. The following dimensionless quantities are imposed:

$$t = \tilde{t} \frac{U_0}{r_0}, \quad r = \frac{\tilde{r}}{r_0}, \quad z = \frac{\tilde{z}}{r_0}, \quad u = \frac{\tilde{u}}{U_0}, \quad w = \frac{\tilde{w}}{U_0}$$

$$p = \frac{\tilde{p}}{\rho U_0^2}, \quad R = \frac{R}{r_0}, \quad \text{Re} = \frac{U_0 r_0 \rho}{\mu}, \quad \text{Fr} = \frac{U_0^2}{g r_0}$$

Equations (3) – (5) are non-dimensionalised and become:

$$r \frac{\partial w}{\partial z} + \frac{\partial(ur)}{\partial r} = 0 \quad (6)$$

$$\frac{\partial u}{\partial t} + \frac{\partial u^2}{\partial r} + \frac{\partial(wu)}{\partial z} + \frac{u^2}{r} = -\frac{\partial p}{\partial r} + \frac{1}{\text{Re}} \left(\frac{\partial^2 u}{\partial r^2} + \frac{1}{r} \frac{\partial u}{\partial r} + \frac{\partial^2 u}{\partial z^2} - \frac{u}{r^2} \right) + \frac{\sin \theta}{\text{Fr}} \quad (7)$$

$$\frac{\partial w}{\partial t} + \frac{\partial(wu)}{\partial r} + \frac{\partial w^2}{\partial z} + \frac{wu}{r} = -\frac{\partial p}{\partial z} + \frac{1}{\text{Re}} \left(\frac{\partial^2 w}{\partial r^2} + \frac{1}{r} \frac{\partial w}{\partial r} + \frac{\partial^2 w}{\partial z^2} \right) - \frac{\cos \theta}{\text{Fr}} \quad (8)$$

where U_0 is the cross-sectional average velocity, r_0 is the non-constricted radius, Re is the Reynolds number and Fr is the Froude number.

Assuming that radial flow does not occur along the symmetry axis of the artery, the normal component of radial velocity and axial velocity gradient of the blood along the axis hence, is presumed to be zero; this means shear stress does not exist. These can be stated mathematically as

$$u(r, z, t) = 0, \quad \frac{\partial w(r, z, t)}{\partial r} = 0 \quad \text{on } r = 0. \quad (9)$$

Blood particles are considered to adhere to inner surface of the vessel. In this case, the velocity boundary conditions on vessel wall obey the no-slip condition and are taken to be

$$u(r, z, t) = \frac{\partial R}{\partial t}, \quad w(r, z, t) = 0 \quad \text{on } r = R(z, t). \quad (10)$$

Next, the inlet velocity conditions are considered to have a parabolic profile which resembles the Hagen-Poiseuille flow through a long circular tube even in unsteady state. It is evident in the two studies by Rappitsch and Perktold [25] and Stangeby and Eithier [26] as:

$$w(r, z, t) = 2U_0 \left(1 - \frac{r^2}{R^2} \right), \quad u(r, z, t) = 0 \quad \text{for } z = 0. \quad (11)$$

At downstream, the velocity is treated to be zero:

$$\frac{\partial w(r, z, t)}{\partial z} = 0 = \frac{\partial u(r, z, t)}{\partial z} \quad \text{for } z = L, \quad (12)$$

where L is the length of the constricted artery segment under study.

Lastly, it is also assumed that no flow takes place when the system is at rest except at the inlet [27], described as:

$$w(r, z, 0) = u(r, z, 0) = p(r, z, 0) = 0 \quad \text{for } z > 0. \quad (13)$$

The solutions procedure to solve the equations (6)-(8) with the boundary conditions (9 - 12) and initial conditions (13) are particularised in [28]. Computation for solving the governing equations is carried out using Matlab programming software. The MAC method algorithm together with pressure-velocity corrections and stability restriction used in this study has been validated by Mustapha et al. [20-22] and Tan & Mustapha [28].

3 Results and Findings

To perform numerical computation implying the considered quantities which have major physiological significances, the following parameters are utilised:

$$k = 0.001; \quad \rho = 1.05 \times 10^3 \text{ kg m}^{-3}; \quad \omega = 2\pi f_p; \quad f_p = 1.2 \text{ Hz}; \quad \phi = 0^0; \quad U_0 = 0.5; \quad \Delta x = 0.02.$$

The non-dimensional length of the artery segment is 64 such that the upstream and downstream lengths are taken to be 10 and 15 respectively. This length is long enough to make sure that the streaming blood has come to a stable condition. Also, to establish numerical results that achieve steady state, the non-dimensional time is taken to be 48. Throughout the current study, value of Froude number which represents the condition of gravitational force is taken to be 0.2.

The first aspect to look at is pressure drop across stenosis along the constricted artery. Figure 3 below shows the dimensionless pressure drop across a 48% occluded mild stenosis verses different values of Reynold's numbers. It shows clearly that with increment of Reynolds number, pressure drop across the vessel decreases. In order to validate the appropriateness of the current model, a comparison is made among the current model with previous work done by Mustapha *et al.* [21], who has modelled blood flow through straight artery segment with 48% occluded single and multiple irregular stenoses respectively. The current model is computed using the value of Froude number $Fr = 0.2$ and inclination of vessel at angle $\theta = 30^\circ$. The main difference of the current model is the addition of gravity term at the momentum equations. By comparing the pressure drop of these three models, it is concluded that the pattern of pressure drop shows acceptable agreement. However, as Reynolds number get higher, current model shows gradual decrement in pressure drop. Meanwhile, the previous models without additional gravity term illustrate that the graph of pressure drop shows drastic continuing decrement.

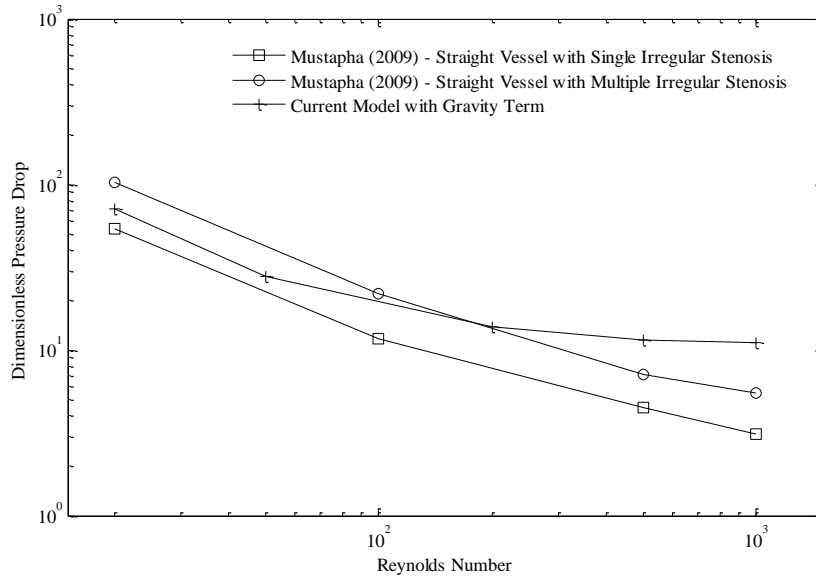


Figure 3: Dimensionless Pressure Drop across a Mild Stenosis (48% Occlusion with $Fr=0.2$) - Comparison with previous work by Mustapha et al. [21]

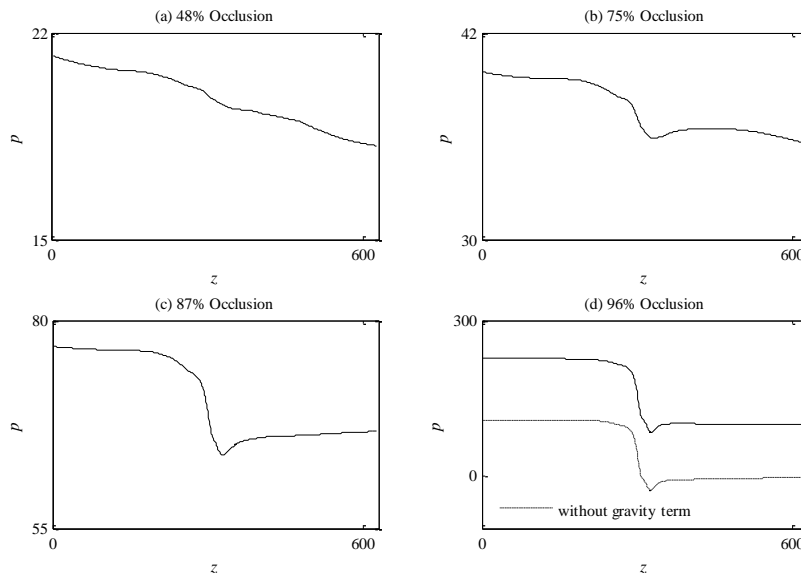


Figure 4: Dimensionless pressure along the Longitudinal Section of Stenosed Arteries with Different Degrees of Stenosis Severities ($Re=200$; $Fr=0.2$).

In Figure 4, pressure along the longitudinal section of stenosed artery is shown. The graphs compare four different stages of severity of stenosis in the vessel. Here, blood is treated as laminar flow, where the value of Reynolds number is taken to be 200. It is clearly observed that the energy difference is very significant through different severity degrees of the stenosis. Under condition of mild stenosis (48% occlusion is taken here), the pressure drop is very slight, where a dimensionless value of 1.8 is observed. However, when compared to severe stenosis (96% occlusion), the dimensionless pressure drop is calculated to be 126.5 which is a significantly large difference.

Next, Figures 5 and 6 exhibit the dimensionless axial velocity versus radial position for the artery segments under different degrees of stenotic occlusion. Streaming blood is assumed to be laminar, where Reynolds numbers here are taken to be 50 and 200 for the graphs respectively. The location of velocity profile is taken at the critical peak of the stenosis, which is at $z=21.8$ cm (refer Figure 2).

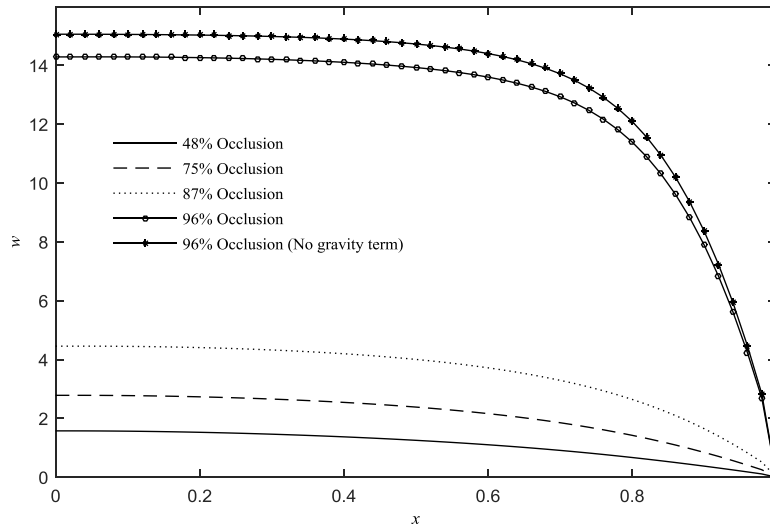


Figure 5: Dimensionless Radial Position vs Dimensionless Axial Position (comparing different severity with $Fr=0.2$ and $Re=50$)

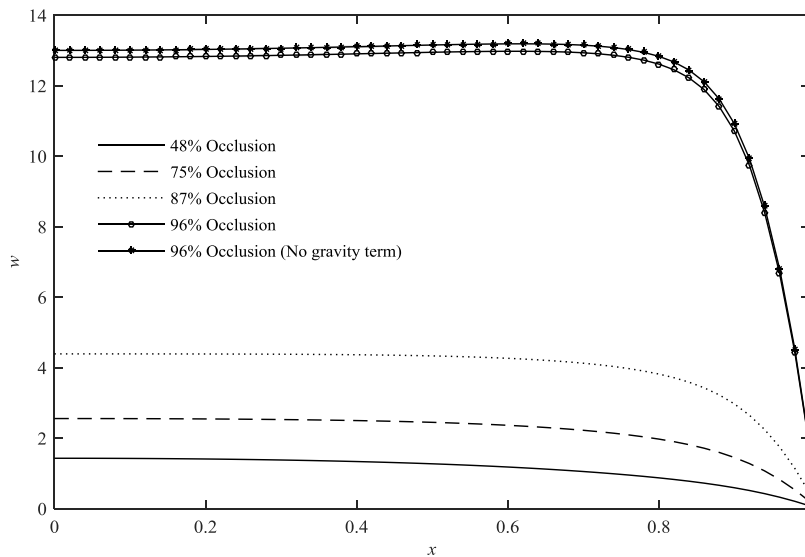


Figure 6: Dimensionless Radial Position vs Dimensionless Axial Position (comparing different severity with $Fr=0.2$ and $Re=200$)

From the figures, velocity values of the blood flow decrease gradually from their individual maximum to zero at the vessel wall. For each case, the velocity decrease gradually from its individual maximum to zero at the vessel wall. As can be seen in both figures, it is significant that the velocity of severe stenosis vessel (96% areal occlusion) is critically the highest compared to segment with milder stenotic vessel at the peak of stenosis. At the same time, from Figures 5 and 6, comparison is also made between dimensionless axial velocity of 96% occlusion model with and without the additional gravity term. The graph clearly shows that the individual maximum of the current model (with additional gravity term) is slightly lower than the one without additional term.

On the other hand, dimensionless centreline velocity of the vessels along the longitudinal direction is also investigated as shown in Figure 7. However, we only compare vessels with severe stenosis, which are 96% and 87% areal occlusions respectively. Even though these two situations differ for only 8% of areal occlusion, the impact is very significant. At the peak of the stenosis, the velocity of vessel with 96% occlusion is obviously much greater than in vessel with 87% occlusion. Next, Figure 8 shows the dimensionless wall shear stress in an artery segment comparing different degree of stenosis severity. The figure is obtained under the same condition which is $Fr=0.2$ and $Re=200$, and

also comparing the wall shear stress with microgravity condition. The wall shear stress profiles give an illustration of stenosis geometry where at the upstream of the stenosis, wall shear stress increases rapidly until the peak of the stenosis. Wall shear stress of each case reaches the critical maximum at critical height of the stenosis and then decrease at the downstream of stenosis.

Furthermore, a comparison is made between the models with and without additional gravity term in the momentum equations, for 48% occlusion case. A slight difference is noticed in the maximum value of wall shear stress.

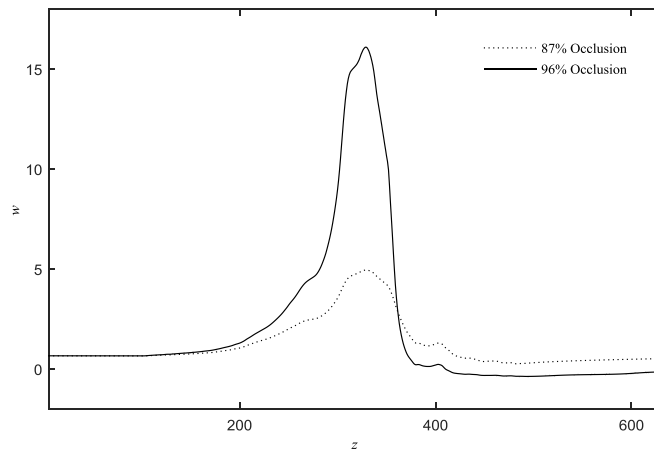


Figure 7: Variation of Axial Velocity at Centreline of Vessel along the Longitudinal Direction

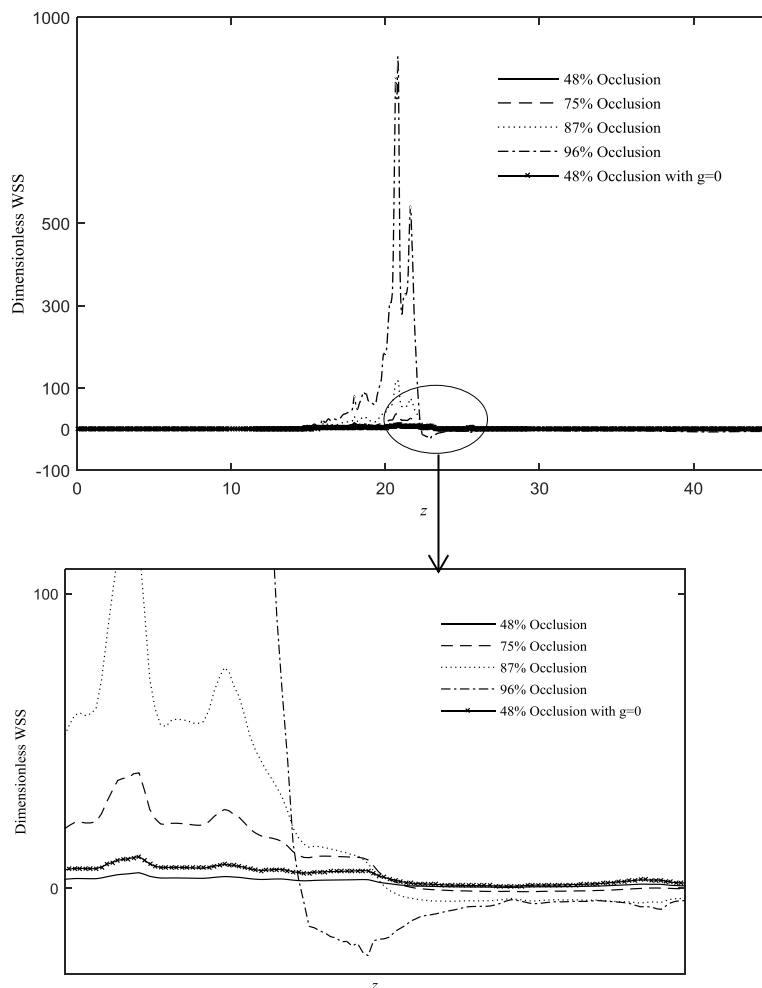


Figure 8: Dimensionless Wall Shear Stress versus Dimensionless Axial Position (comparing different severity with $Fr=0.2$ and $Re=200$)

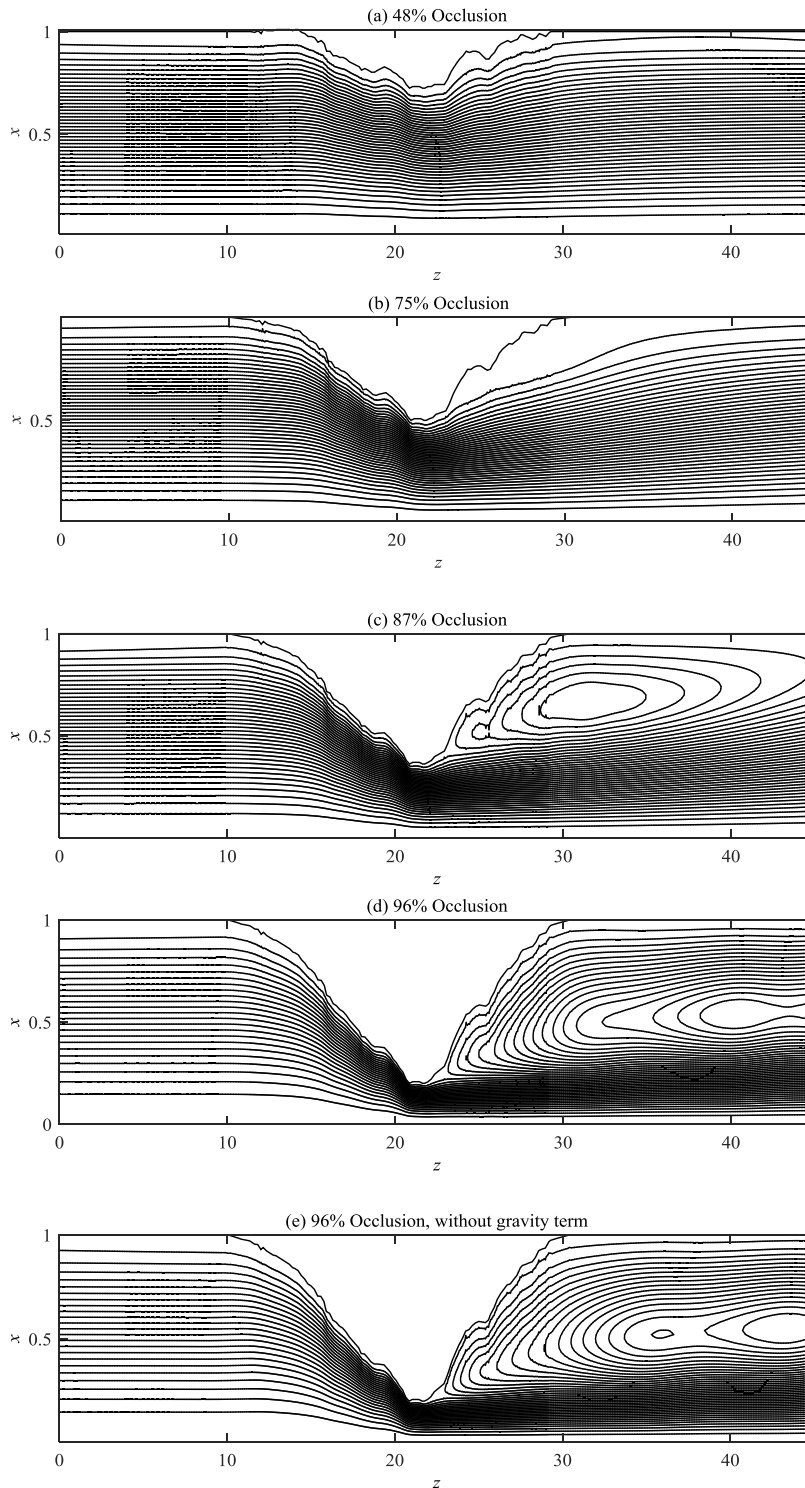


Figure 9: Variations of Streamlines

Figure 9 exhibits streamlines for the considered four stages of stenosis severity, which are 48%, 75%, 87% and 96% occlusion respectively. For cases of 48% and 75%, no separation of flow is noticed. However, significant flow separation occurs in both 87% and 96% stenosis cases, which locates immediately after the stenotic region. Besides, comparison is also made between the current model (with gravity) and the previous model (without gravity) for the 96% areal occlusion vessel. There is noticeable difference at the pattern of flow separation after the stenotic throat.

4 Discussion

Among the factors affecting pressure drop across stenosis in a constricted vessel are stenosis severity and Reynolds number. Pressure drop over a stenosed vessel occurs because of energy difference before and after stenosis where blood flow accelerates through stenosis [20]. At a condition of low Reynolds number, blood is comparatively less turbulence; hence, the effects of energy difference are more significant. Pressure drop data is useful and associable to help finding fractional flow reserve (FFR) across a specific constricted vessel, where treatment can be decided accordingly. However, further studies need to be carried out in order to overcome some limitations of the current model, especially the determination of initial pressure of each individual vessel, to ensure its accuracy. Besides, results also show that different severity of similar shaped stenosis gives very different pressure drop patterns and velocity profiles (refer Figure 4 to Figure 7). When stenosis becomes severe, streaming blood encounters extreme high velocity to pass through the thin throat of vessel lumen. Apparently, shape and areal occlusion of a stenosis should be taken into consideration during modelling since a little change of stenosis occlusion percentage can bring serious impact on flow pattern. Also, a severe stenosis can turn out high pressure in a vessel, which would also increase the pace of heart beat. This could further induce hypertension, high blood pressure or heart related problems in human body.

Further, when discussing from the perspective of wall shear stress, severe stenosis blocks almost the whole vessel lumen and hence, wall shear stress for the constricted segment is extremely high. However, proximal downstream shows a significant reduction of wall shear stress. As matched in the variations of streamline (Figure 9), it is observed that recirculation and flow separations occur at the proximal downstream of stenosis also. Such low shear stress areas tend to promote further deposition of stenotic plaques [29]. When stenosis reaches severe state, the reduction of wall shear stress at its proximal downstream becomes more significant, and thus, pace of further plaque deposition would also become quicker.

On the other hand, among the results, comparison is also made between the current model and the previous model, which are with and without the additional of gravity term respectively. Apparently the additional term is significant to influence the numerical algorithms and results; hence, it is suggested that gravity term shall be considered in future studies on blood flow.

5 Conclusion

This paper presented the investigation on effects of stenosis severity on blood flow through artery. The model used in this study is an unsteady two dimensional nonlinear model with additional term of gravitational force at the momentum equations. Geometry of the blood vessel is chosen to be a single axisymmetric tube of artery with an irregular stenosis, comparing different percentage of stenosis occlusion. Streaming blood in the artery is considered as laminar incompressible Newtonian fluid. The governing equations are non-dimensionalised and transformed using radial transformation. Then, they are solved using the finite difference approximations based on Marker and Cell (MAC) method. Values of gravitation is described dimensionlessly via Froude number. Lower value of Froude number represents a condition with higher gravitational force and vice versa. The Froude number chosen in this study is $Fr=0.2$, and the Reynold's number chosen is $Re=200$ to compare among different level of stenotic severity. From the results, slight difference of occlusion percentage can lead to significant impact on blood flow patterns and consequenses.

For further researches, gravity term shall always be considered in the governing equations. Further studies will also be done by treating blood as different kinds of non-Newtonian fluids. Besides, model of the vessel can be improved by changing the vessel geometry profiles, which would be closer to clinical cases in real life.

Acknowledgment

The first author would like to thank the Ministry of Higher Education Malaysia for financial support under MyBrain15.

References

- [1] Glenny, R.W., Bernard, S., Robertson, H.T., and Hlastala, M.P., Gravity is an important but secondary determinant of regional pulmonary blood flow in upright primates. *J. Appl Physiol.* 1999. 86 : 623-32.
- [2] Michels, D. B., and West, J. B., Distribution of pulmonary ventilation and perfusion during short periods of weightlessness, *J. Appl. Physiol.* 1978. 45 : 987–998.
- [3] West, J. B., Dollery, C. T., Matthews, M. E, and Zardini, P., Distribution of blood flow and ventilation in saline-filled lung. *J. Appl. Physiol.* 1965. 20 : 1107–1117.
- [4] Kim C.S., Kiris C, Kwak D and David T., Numerical Simulation of Local Blood Flow in the Carotid and Cerebral Arteries under Altered Gravity. *J. Biomech Eng.* 2006. 128: 194-202.
- [5] Payne S.J., Analysis of the effects of gravity and wall thickness in a model of blood flow through axisymmetric vessels. *Med. Biol. Eng. Comput.* 2004. 42: 799-806.
- [6] Burrowes, K.S., Hunter, P.J. and Tawhai, M.H., Investigation of the Relative Effects of Vascular Branching Structure and Gravity on Pulmonary Arterial Blood Flow Heterogeneity via an Image-based Computational Model. *Aca Radiol.* 2005. 12 : 1464-1474.
- [7] Burrowes, K.S. and Tawhai M.H., Computational predictions of pulmonary blood flow gradients: Gravity versus structure. *Resp Physiol & Neurobio.* 2006. 154 : 515-523.
- [8] Boynton R. *Precise Measurement of Mass.* Texas: Lamentation Mountain Press. 2001.
- [9] Ku, D.N., Blood Flow in Arteries, *Ann Rev Fluid Mech*, 1997. 29 : 399-434.
- [10] Mandal, P.K., Chakravarty, S., Mandal, A and Amin, N., Effect of Body Acceleration on Unsteady Pulsatile Flow of Non-Newtonian Fluid through a Stenosed Artery, *Appl Math Comput*, 2007. 189. 766-779.
- [11] Berbich, L., Bensalah, A., Fludad, P. and Benkirane, R., Non-linear Analysis of the Arterial Pulsatile Flow: Assessment of a Model Allowing a Non-invasive Ultrasonic Functional Exploration. *Med Eng & Phys*, 2001. 23:175-183.
- [12] Deplano, V., Bertolotti, C. and Boiron, O., Numerical Simulation of Unsteady Flows in a Stenosed Coronary Bypass Graft, *Med. Biol. Eng. Comput.*, 2001. 39:488-499.
- [13] Ling S.C. and Atabek, H.B., A Nonlinear Analysis of Pulsatile Flow in Arteries, *J. Fluid. Mech.*, 1972. 55: 493-511.
- [14] Padmanabhan, N., Mathematical Model of Arterial Stenosis, *Med. & Biol. Eng. & Comput.* 1980.18:281-286.
- [15] Back, L.H., Cho, Y.I., Crawford D.W. and Cuffel, R.F., Effect of mild atherosclerosis on flow resistance in a coronary artery casting of man. *ASME J. Biomech. Eng.*, 1984. 106 : 48-53.
- [16] Johnston P.R. and Kilpatrick, D., Mathematical modelling of flow through an irregular arterial stenosis. *J. Biomech.*, 1991.24: 1069-1077.
- [17] Chakravarty, S. and Sannigrahi, A.K., Effects of body acceleration on Blood Flow in an Irregular Stenosed Artery, *Mathl. Comput. Model.* 1994. 19 : 93-103.
- [18] Jung, H., Choi, J.W. and Park, C.G., Asymmetric Flows of Non-Newtonian Fluids in Symmetric Stenosed Artery, *Korea-Australia Rheol J.* 2004. 16 : 101-108.
- [19] Mandal, P.K., An Unsteady Analysis of Non-Newtonian Blood Flow through Tapered Arteries with a Stenosis, *Int J. Non-Linear Mech.* 2005. 40: 151-164.
- [20] Mustapha, N, Chakravarty, S., Mandal, P.K. and Amin, N. Unsteady Response of Blood Flow through a Couple of Irregular Arterial Constrictions to Body Acceleration. *J. of Mech Med & Bio.* 2008. 8: 395-420.
- [21] Mustapha, N., Amin, N., Chakravarty, S. and Mandal P.K., Unsteady magnetohydrodynamic blood flow through irregular multi-stenosed arteries. *Comp Bio & Med.* 2009. 39: 896-906.
- [22] Mustapha, N., Mandal, P.K., Johnston, P.R. and Amin, N. A numerical simulation of unsteady blood flow through multi-irregular arterial stenoses. *Appl Math Model.* 2010. 34: 1559-1573.

- [23] Neal, G.U., Jacques, A.M., Bruyne, B.D., William, W., Thierry, B. and Paolo, G.C., Relation between Myocardial Blood Flow and the Severity of Coronary Artery Stenosis. *The New England J Med.* 1994. 330 : 1782-1788.
- [24] Gaskell PH, Jimack PK, Sellier M, Thompson HM and Wilson MCT. Gravity-driven flow of continuous thin liquid films on non-porous substrates with topography. *J. Fluid Mechs.* 2004. 509 : 253-280.
- [25] Rappitsch, G. and Perktold, K., Computer simulation of convective diffusion processes in large arteries. *J. Biomech. Eng.* 1996. **29** : **207-15**.
- [26] Stangeby D.K. and Eithier, C.R. Computational analysis of coupled blood wall arterial LDL transport. *J. Biomech Eng.* 2002. 124: 1-8.
- [27] Tu, C., Deville, M., Dheur, L. and Vanderschuren, L., Finite element simulation of pulsatile flow through arterial stenosis. *J. Biomech.* 1992. 25: 1141-1152.
- [28] Tan, Y.B. and Mustapha, N. Numerical Modeling of Blood Flow in Irregular Stenosed Artery with the Effects of Gravity. *J. Teknologi (Sciences & Engineering)*. 2013. 62: 57-64.
- [29] Papaioannou, T.G. and Stefanadis, C. Vascular Wall Shear Stress: Basic Principles and Methods. *Hellenic J. Cardiol.* 2005. 46 : 9-15.